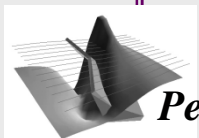


# Application of 3D CSAMT Inversion to Various Data Components and Its Enhancement

*Ruizhong Jia\*, R.W. Groom, Petros Eikon Inc. , Ontario, Canada*

## TOPICS

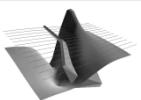
- **Forward simulation**
- **A trust-region inversion technique**
- **First Synthetic Example**
- **Second Synthetic Example**
- **Inversion with striking and dipping grid cells**
- **A real data example**
- **Conclusions and Future Work**



*Petroseikon*

# Forward simulation

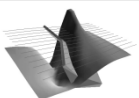
- The algorithm is not limited by assumption regarding the farfield. **Take into consideration of the TX current bipole geometry.**
- utilize a controlled source approach utilizing the specifics of the grounded transmitter incorporating not only the injected currents but also the induced fields from the transmitted magnetic fields.
- Based on a Localized Non-Linear (LN) approximator in (Habashy et al, 1993) and (Murray et al, 1999) when scattering is controlled principally by either injected or induced currents in the host structures.
- The technique is efficient and stable in simulating three-dimensional electromagnetic scattering



# Inversion technique

## - a constrained trust-region method

- solves a least-squares minimization problem with simple bound constraints and has a fast rate of convergence.
- a quadratic model within a region, defined by the trust-region radius, is trusted to be an adequate representation of the objective function. The trust-region method then calculates the step to the approximate minimum of the model in this region.
- We utilized a projected gradient method to determine an initial point with sufficient reduction of the quadratic model. The projected gradient method is more efficient as several bound constraints can be added simultaneously.
- As the second stage of the step computation, a further reduction of the quadratic model is sought to enhance the convergence of the inversion with the additional restriction that the bounds on the parameters are kept fixed throughout the second process.



# Objective function

minimize  $\phi = \phi_d + \mu\phi_m$

$\vec{K} = (\rho_1, \rho_2, \dots, \rho_M)^T$  resistivity model vector

Constraints:  $l_i \leq \rho_i \leq u_i$

$\vec{d}_0 = (d_1^0, d_2^0, \dots, d_N^0)$  observed data

$\vec{d} = (d_1, d_2, \dots, d_N)$  predicted data

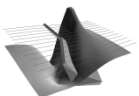
$\phi_d = \left\| W_d (\vec{d} - \vec{d}_0) \right\|^2$  data misfit

$W_d = \text{diag}(1/\sigma_1, 1/\sigma_2, \dots, 1/\sigma_N)$

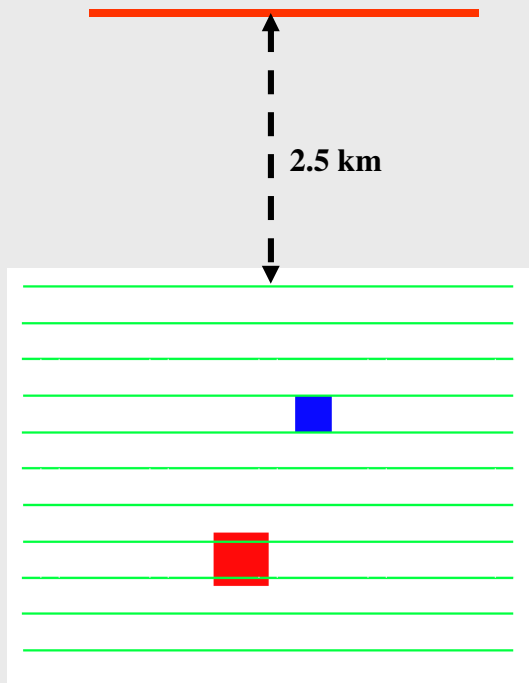
$\sigma_i$  is the standard deviation of the  $i$ -th datum

$\mu$  is a regularization parameter

$\phi_m$  measures the smoothness of the resistivity distribution



# First synthetic example -Survey configuration

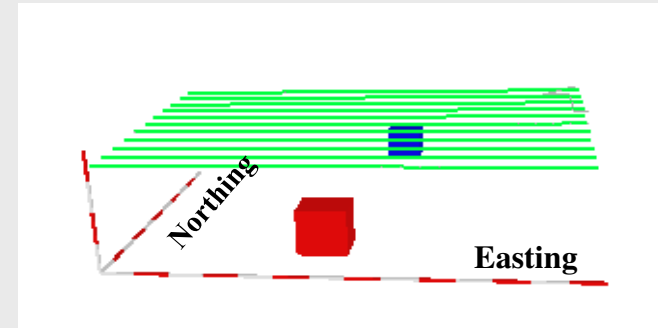


**Survey area:** 1350 x 1000 m, 11 lines, 308 stations

**Station separation:** 50 m

**Line spacing:** 100 m

Transmitter is 2.5 km from the survey area  
and has a length of 1 km



**model properties:**

**Body 1**

**Dimension:** cube of side 150 m

**Depth to top:** 200 m

**resistivity :** 2  $\Omega\text{m}$

**Body 2**

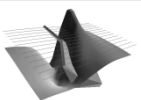
**Dimension:** cube of side 100 m

**Depth to top:** 50 m

**resistivity :** 1000  $\Omega\text{m}$

**Background layered earth model:**

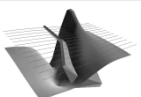
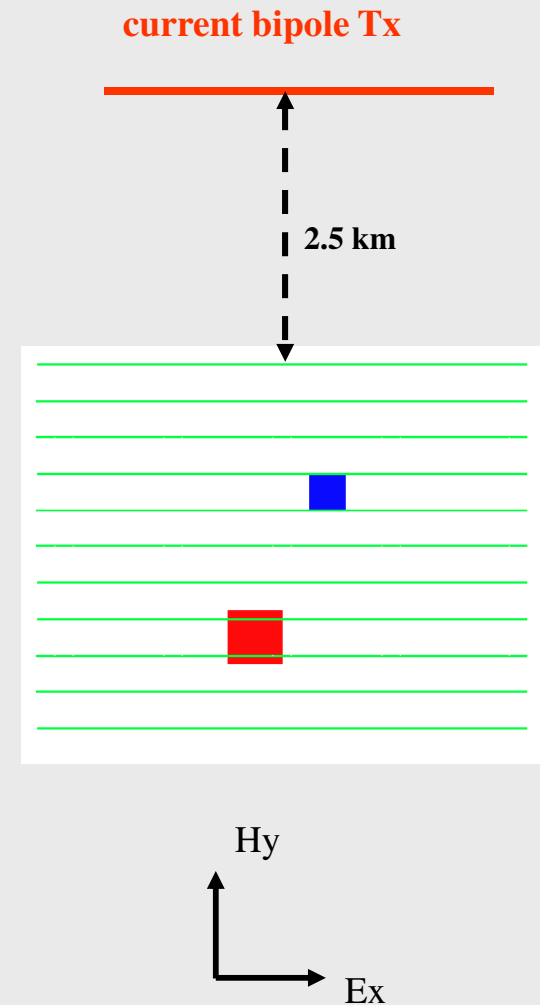
uniform 100  $\Omega\text{m}$



# Synthetic data generation

- Simulated  $E_x$  and  $H_y$
- 3 frequencies (Hz): 16, 64, 512
- $E_x$ : simulated with voltage bipole of length 50 m
- The simulated data were added noise of 2% of the datum magnitude

Computed impedance:  $Z_{xy} = \frac{E_x}{H_y}$



# Inversion setting

## -regular grid

**3D inversion region: 1600 x 1300 x 600 m**

**Grid cell size: 50 x 50 x 50 m**

**Grid cell number: 32 x 26 x 12**

**Starting model:** uniform half-space of 100  $\Omega\text{m}$

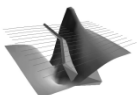
**Constraints:**  $1 \leq \rho_i \leq 100 \quad \Omega\text{m}$

**3 Frequencies used (Hz): 16, 64, 512**

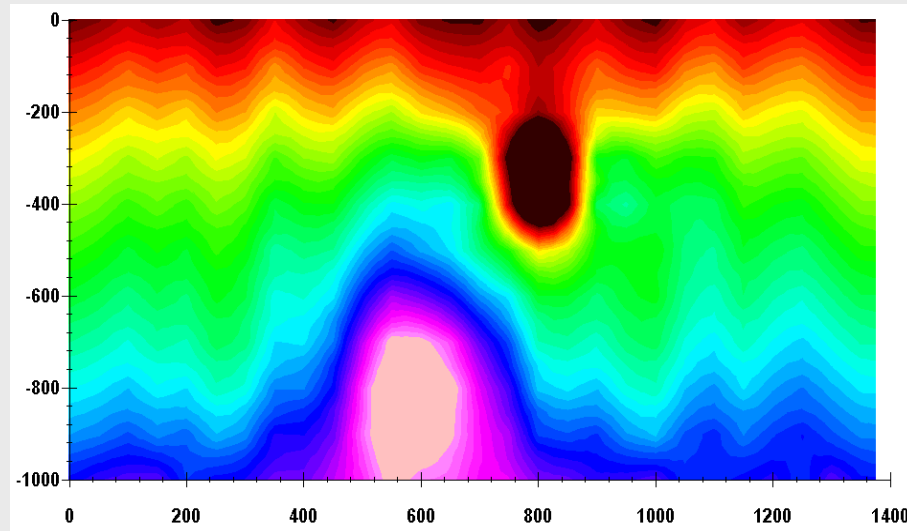
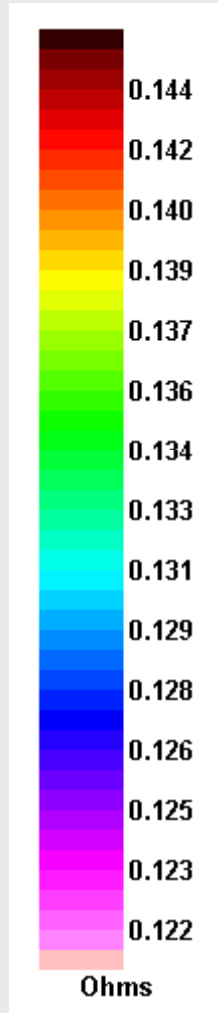
**smoothing coefficients:**

EW: 3, NS: 3, Vertical: 8

Inversion on apparent resistivity and phase



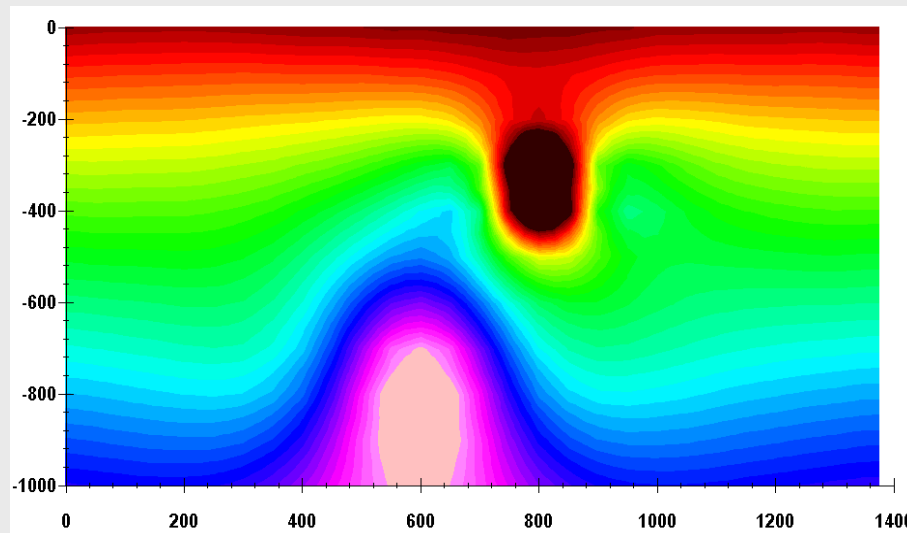
# Gridded predicted data VS "true" data



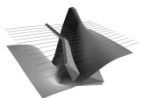
"true" data

16 Hz data

Apparent resistivity

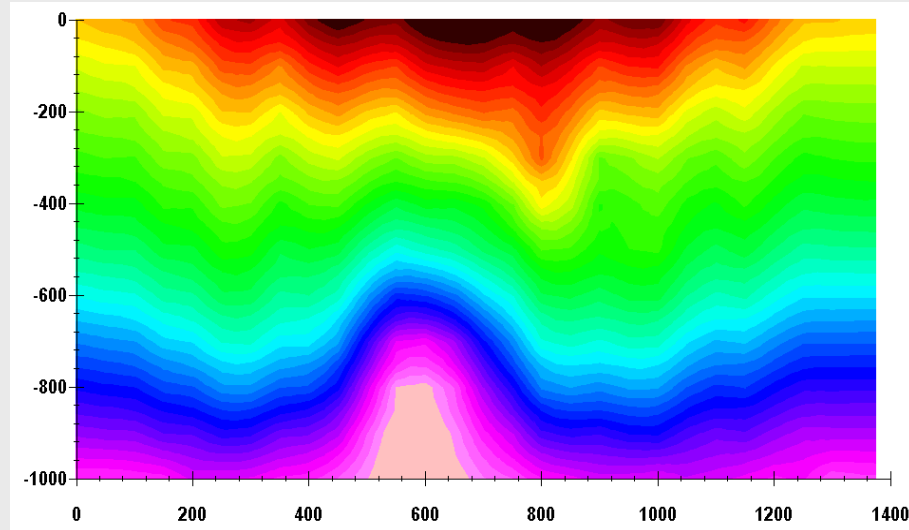
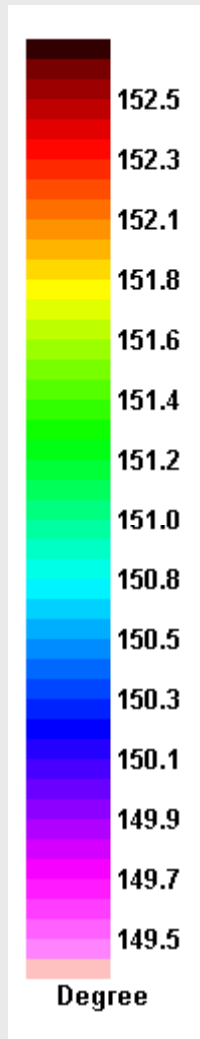


predicted data





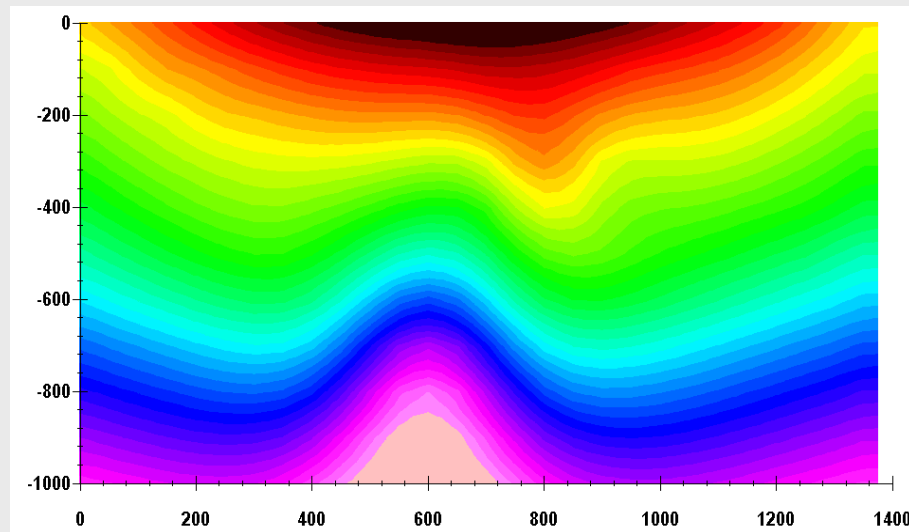
# Gridded predicted data VS "true" data



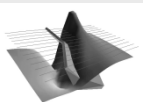
"true" data

16 Hz data

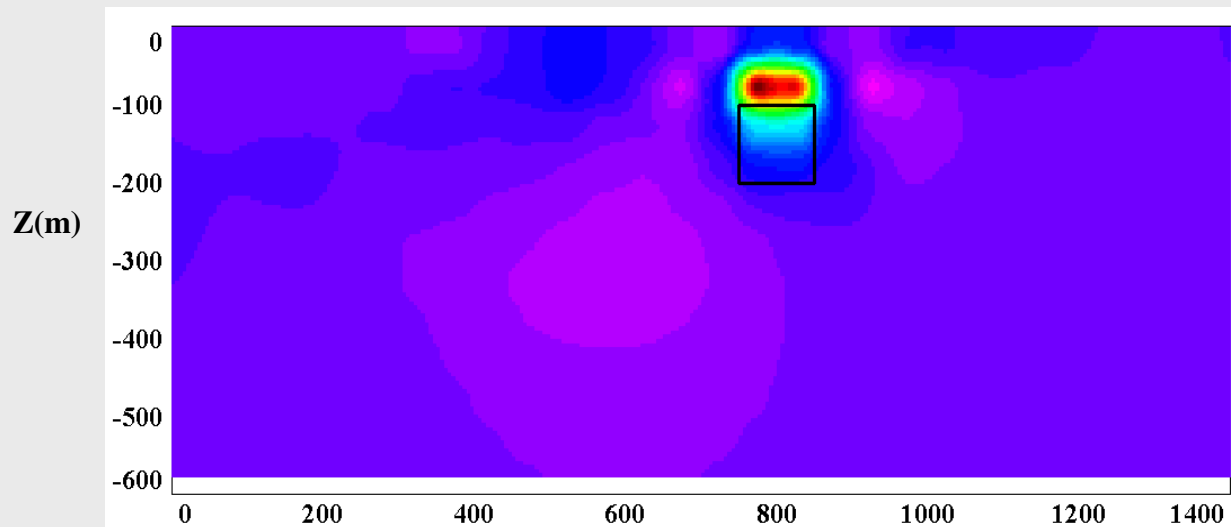
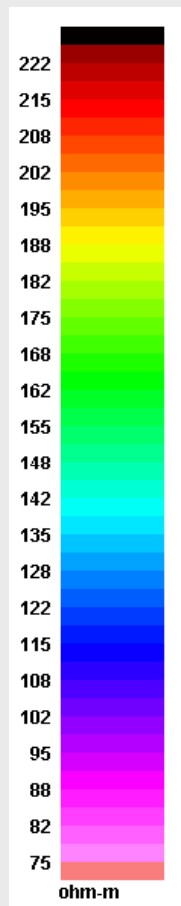
phase



predicted data

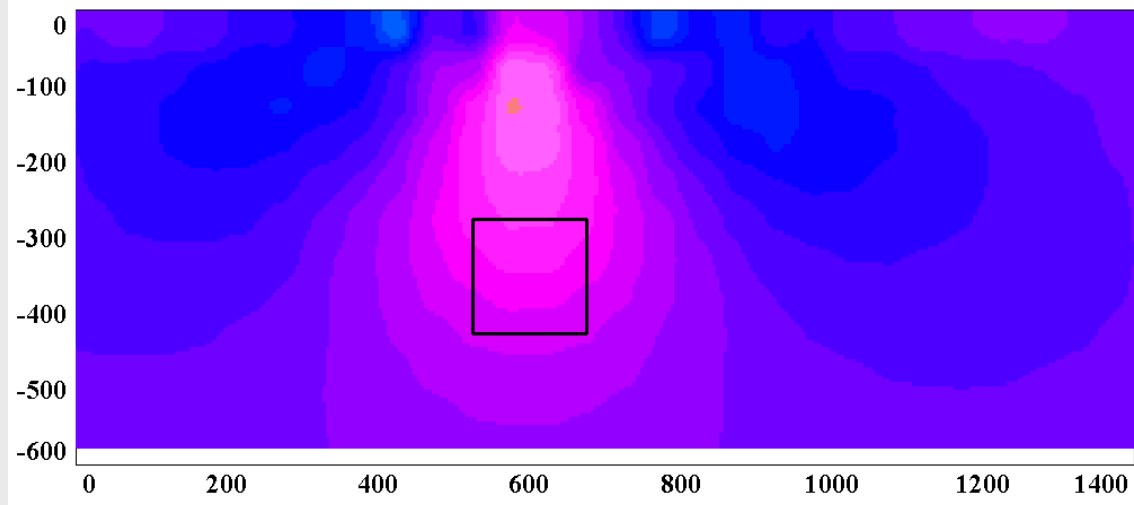


# Recovered model



slice at  
 $y = -350$

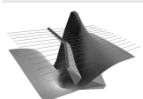
through the  
center of Body 2



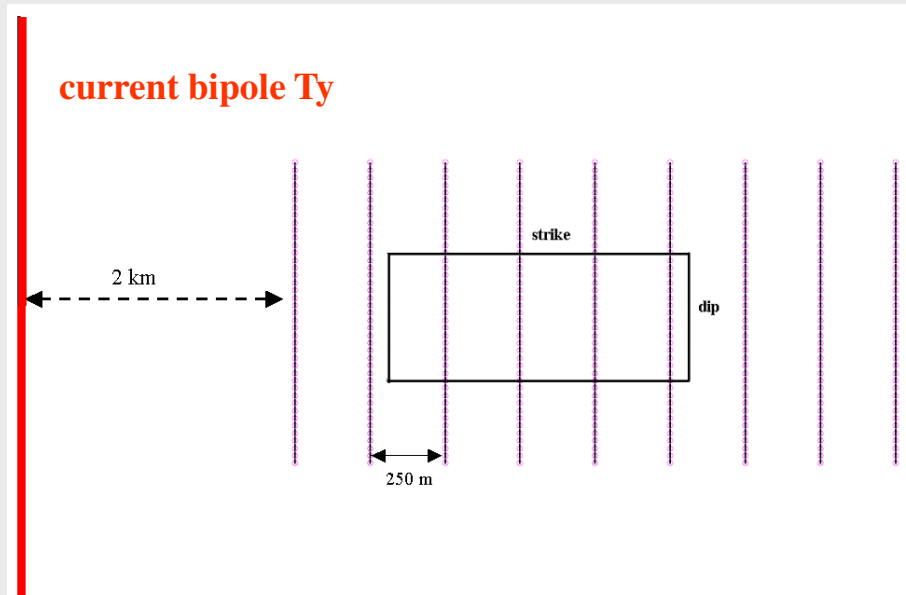
slice at  
 $y = -750$

through the  
center of Body 1

Easting (m)

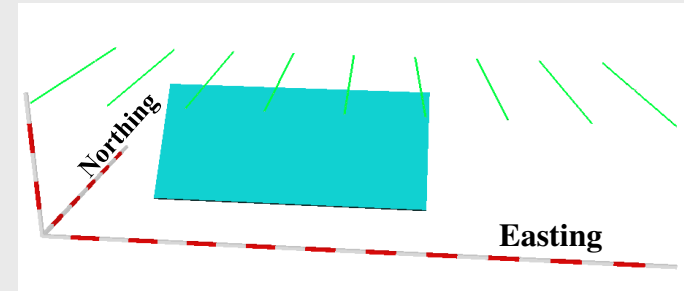


# Survey configuration



Transmitter is 2km from the survey area and has a length of 2km

**Background layered earth model:**  
uniform 1000  $\Omega\text{m}$



**Survey area:** 2000 x 1000 m, 9 lines, 369 stations

**Station separation:** 25 m

**Line spacing:** 250m

**model properties:**

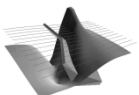
**slab-type anomaly:** 1000 x 500 x 10 m,

**Dipping:** 45 degrees

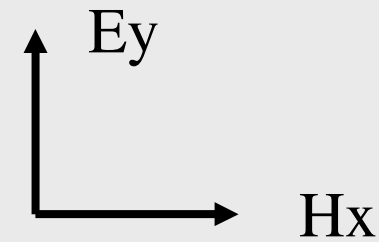
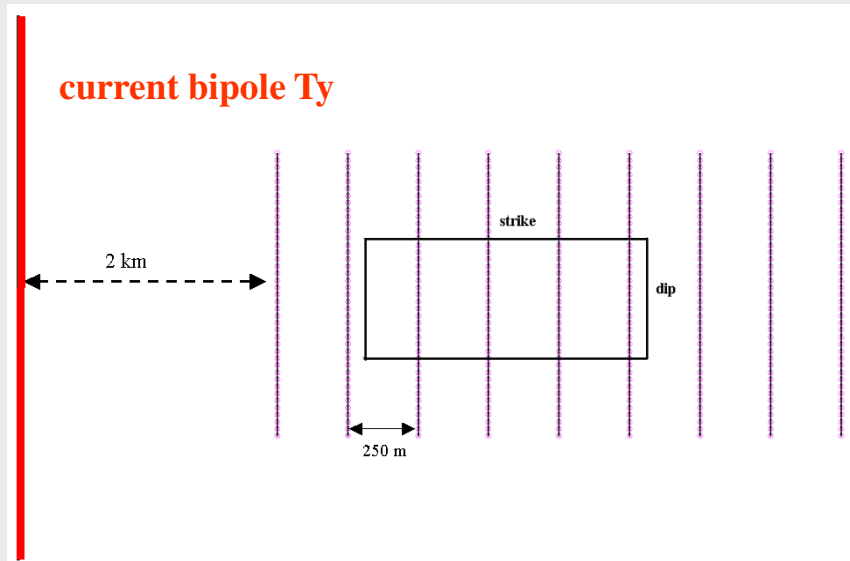
**Striking:** east-west

**Depth to top:** 75 m

**resistivity :** 10  $\Omega\text{m}$

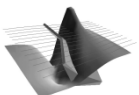


# Synthetic data generation



- Simulated  $E_y$  and  $H_x$
- 9 frequencies (Hz): 1, 10, 60, 100, 600, 1k, 3k, 6k, 10k
- $E_y$ : simulated with voltage bipole of length 50 m
- The simulated data were added noise of 3% of the datum magnitude

Computed impedance: 
$$Z_{yx} = \frac{E_y}{H_x}$$



# Inversion setting

## -regular grid

**3D inversion region: 2200 x 1100 x 600 m**

**Grid cell size: 125 x 25 x 50 m**

**Grid cell number: 18 x 44 x 12**

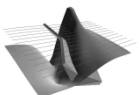
**Starting model:** uniform half-space of 1000  $\Omega\text{m}$

**Constraints:**  $1 \leq \rho_i \leq 1000 \Omega\text{m}$

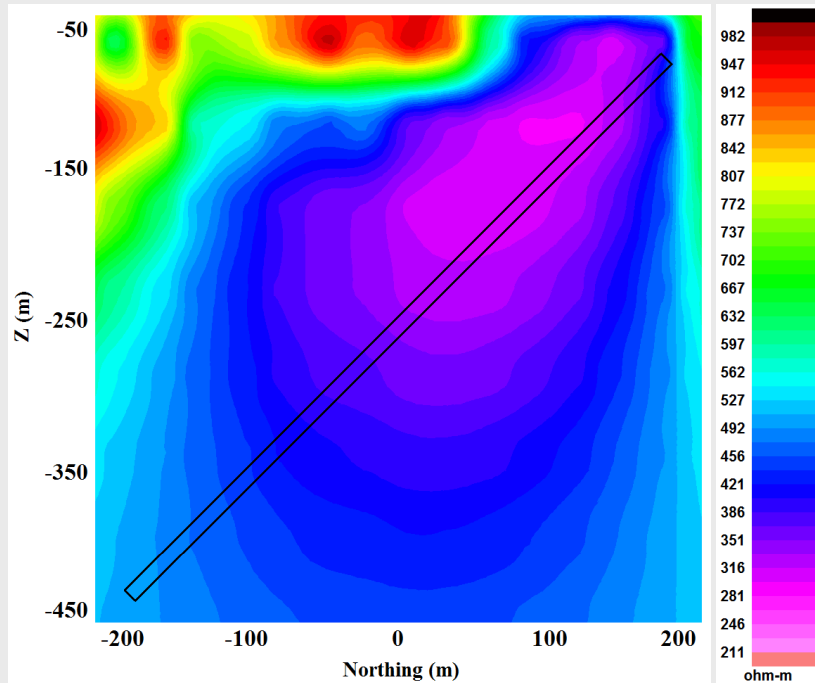
**9 Frequencies used (Hz):** 1, 10, 60, 100, 600, 1k, 3k, 6k, 10k

**smoothing coefficients:**

EW: 3, NS: 0.1, Vertical: 8

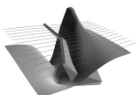


## Recovered model – electric field inversion

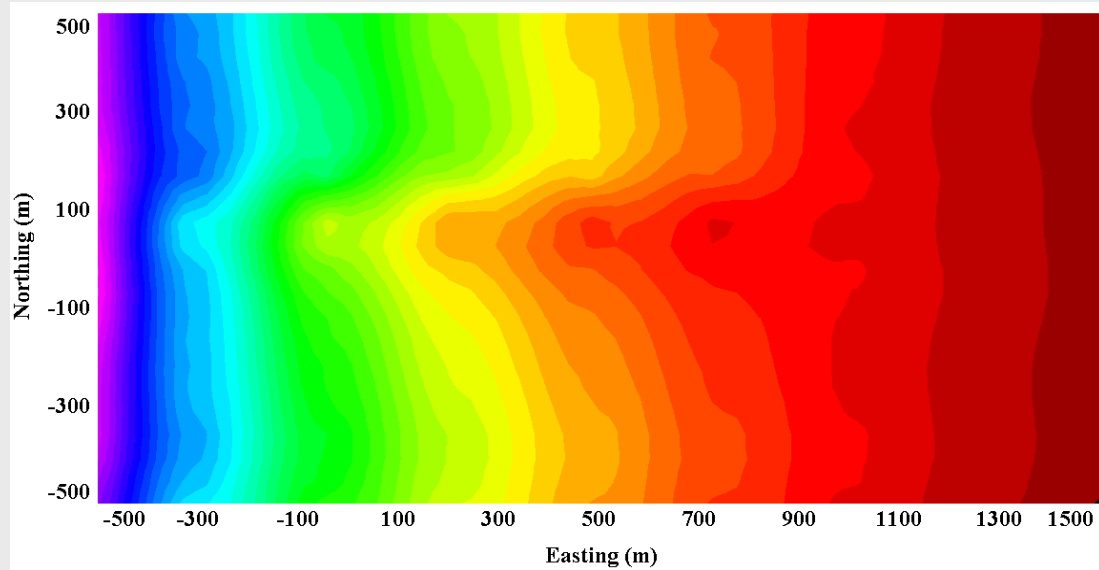
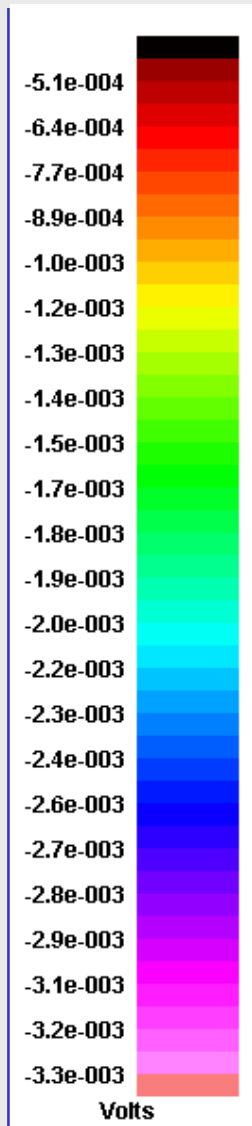


vertical slice of the inverted model through the center of the true model (at  $x = -50$ )

The conductive features in the inverted resistivity distribution models outline a dipping structure, although becoming smooth and broad at greater depths.



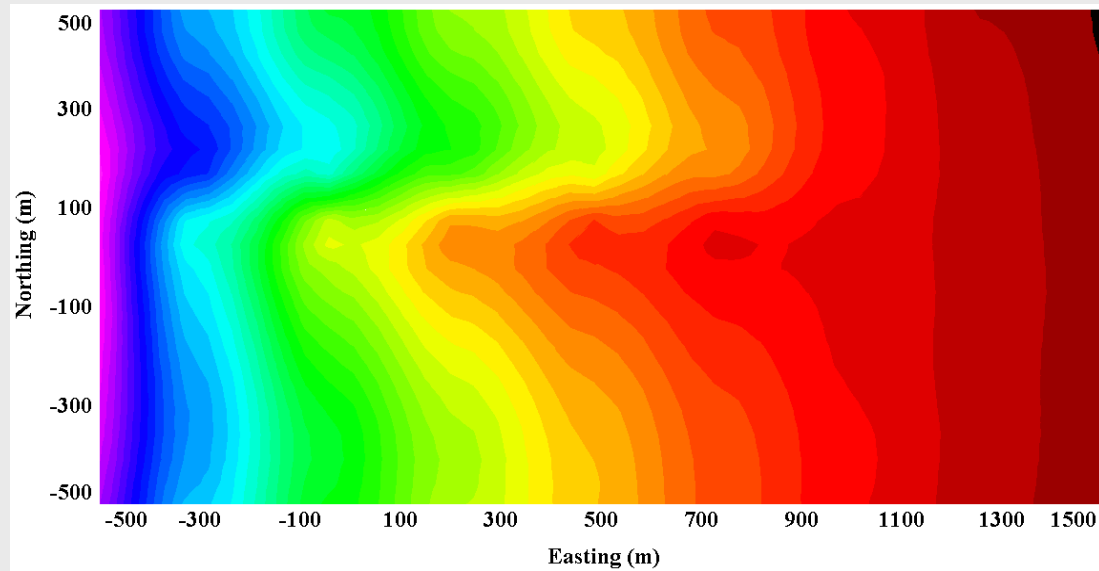
# Gridded predicted data VS “true” data



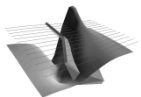
*"true" data*

1 kHz data

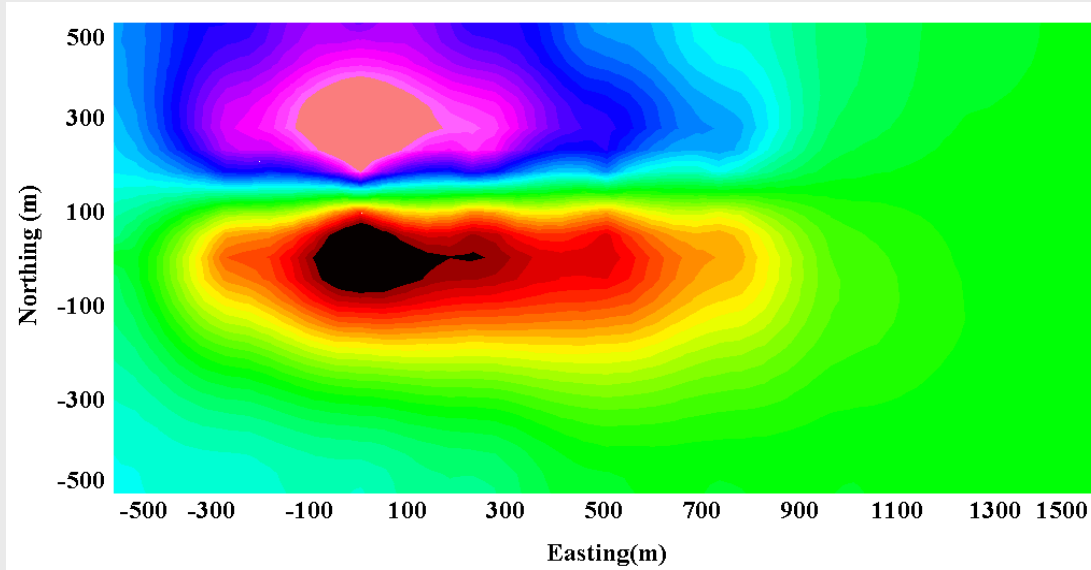
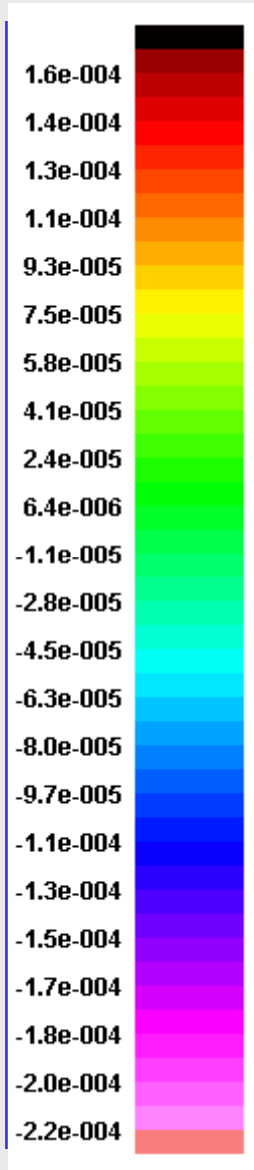
real part



predicted data



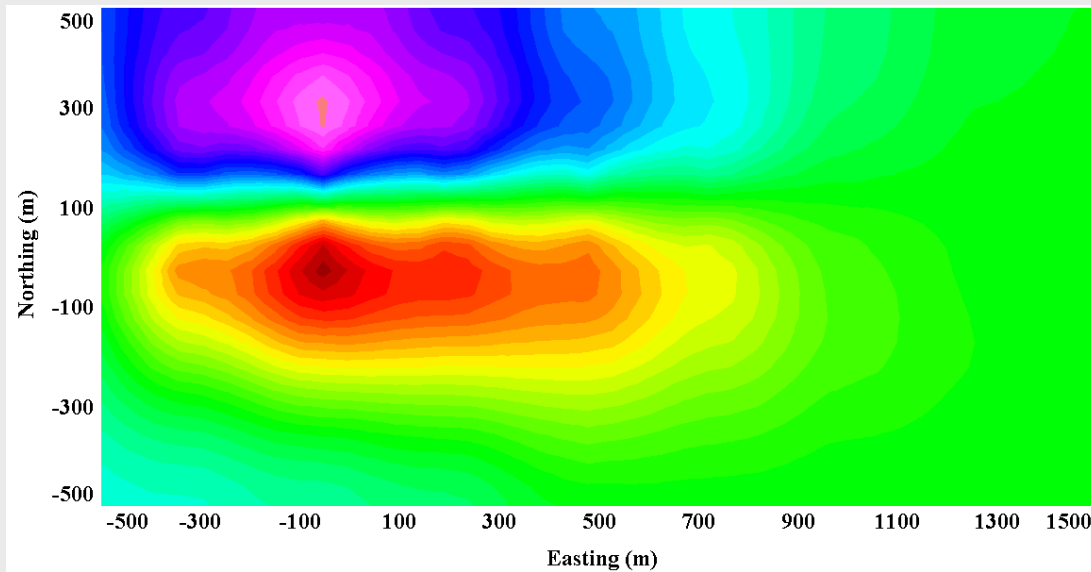
# Gridded predicted data VS “true” data



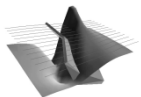
*”true” data*

1 kHz data

Imaginary part



predicted data



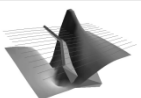
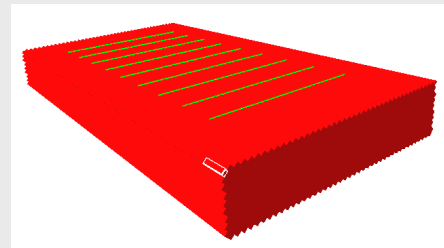


# Incorporating known strike and dip into inversion

- Assume that the strike and dip of linear structures are known.
- Build a 3D mesh model according to the strike and dip
- grid cells are oriented along known strike and dip directions
- Find the resistivity distribution of the 3D mesh model.

## The advantages of utilizing dipping grid cells:

- Make it easy to impose smoothing constraints along the known strike and dip direction.
- It can also improve the recovered model resolution as a dipping linear structure can be better represented with the grid cells of the same orientation.



# Dipping grid inversion setting

- 3D inversion region: 2200 x 1100 x 600 m
- Each cell strikes EW and dips 45° to the south
- Grid cell size: strike length of 125 m, an extent down dip 50 m, thickness 25 m
- Grid cell number: 18 x 44 x 17

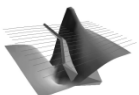
**Starting model:** uniform half-space of 1000  $\Omega\text{m}$

**Constraints:**  $1 \leq \rho_i \leq 1000 \Omega\text{m}$

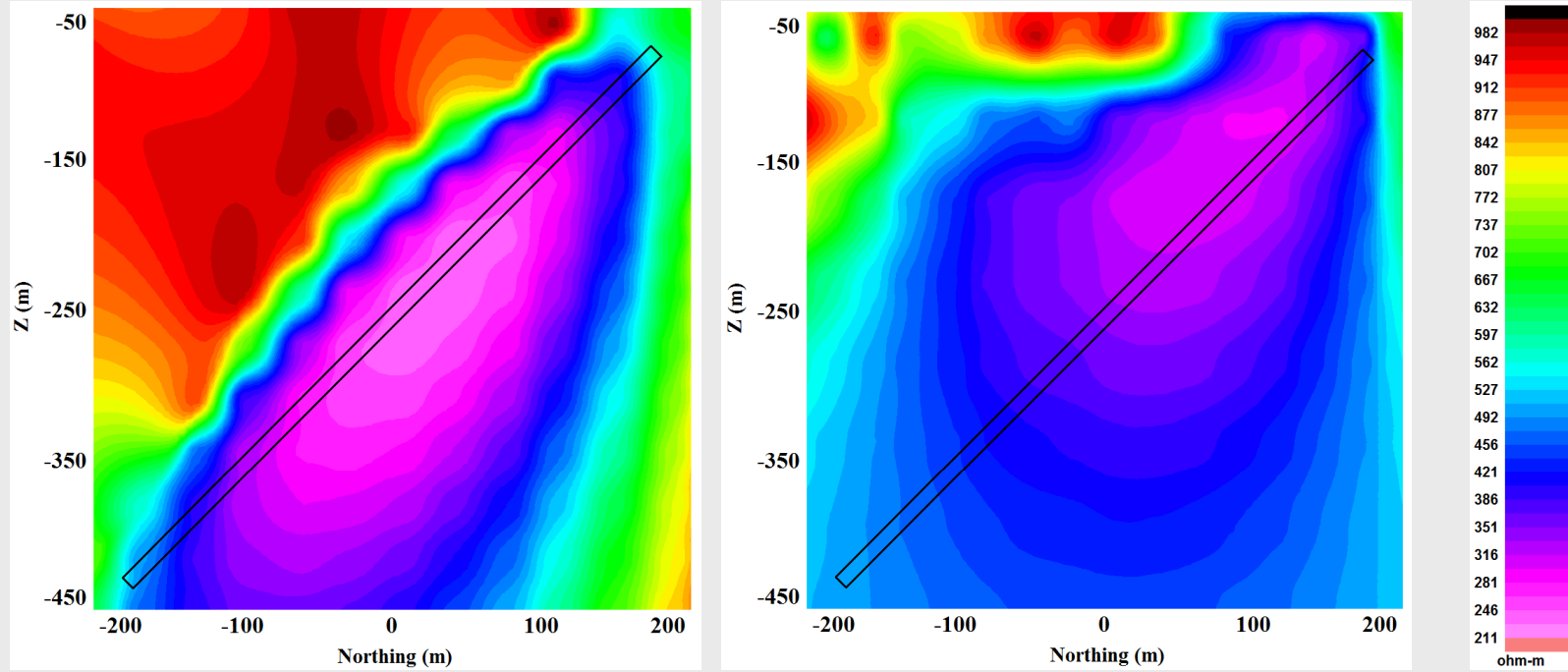
**9 Frequencies used (Hz):** 1, 10, 60, 100, 600, 1k, 3k, 6k, 10k

**smoothing coefficients:**

3 in Strike (EW), 0.1 NS, 8 in dip direction

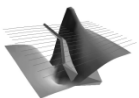


# Recovered model from dipping grid inversion



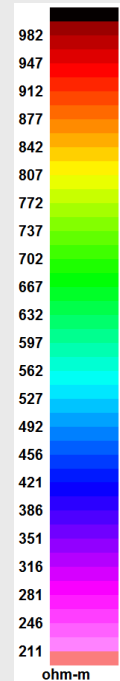
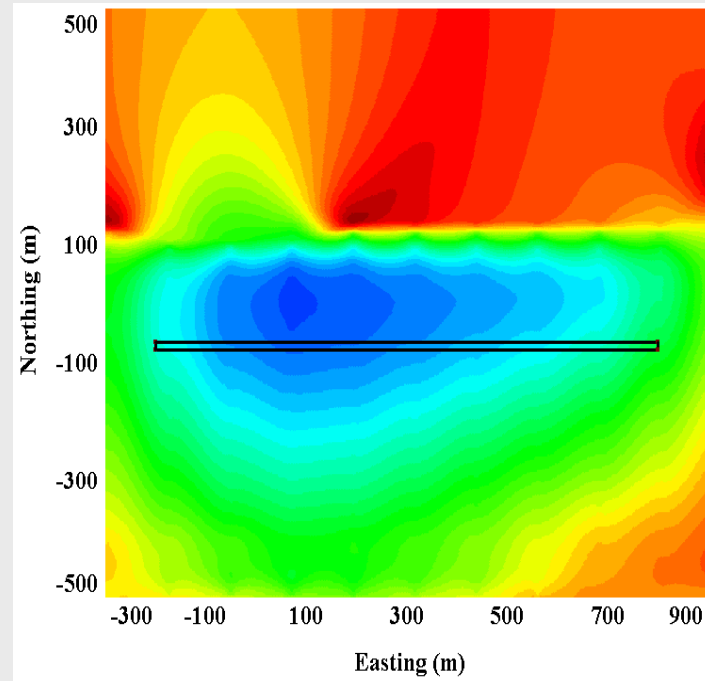
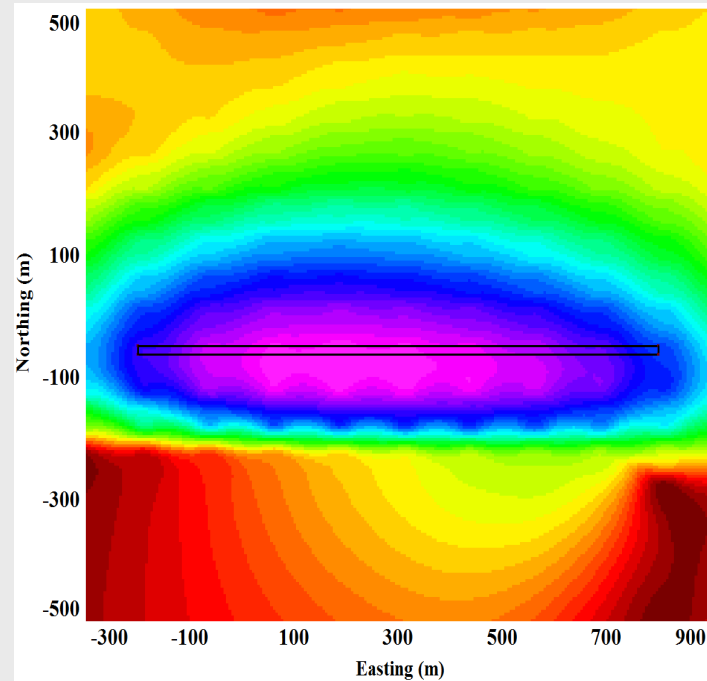
vertical slice of the inverted model through the center of  
the true model (at  $x = -50$ )

the inverted model with a dipping grid demonstrates a better recovery  
of the structure with higher resolution, particularly at depth



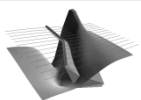
# Recovered model

slice at depth 300 m

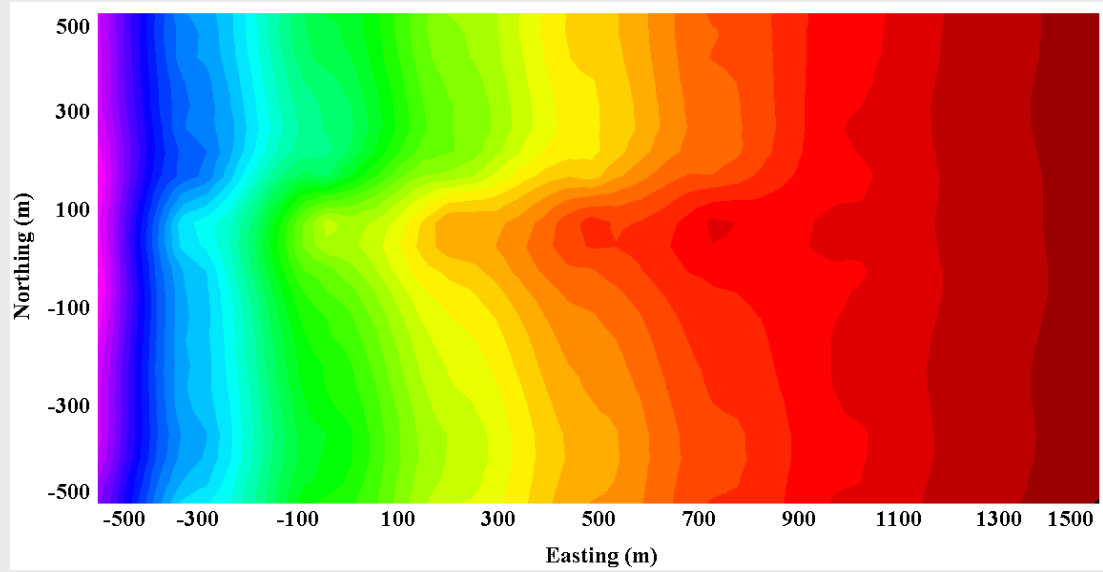
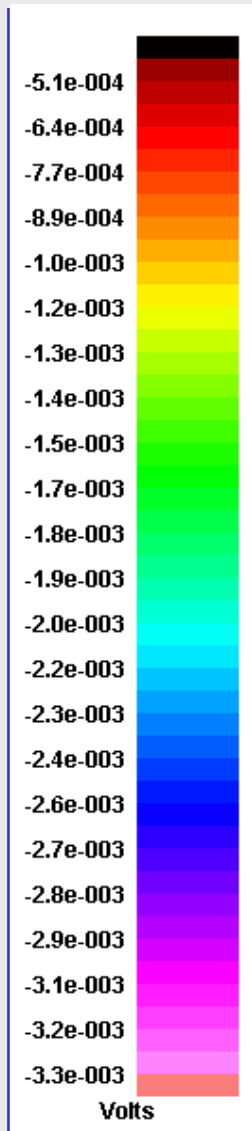


slice at depth 300 m

the inverted model with a dipping grid demonstrates a better recovery of the structure with higher resolution



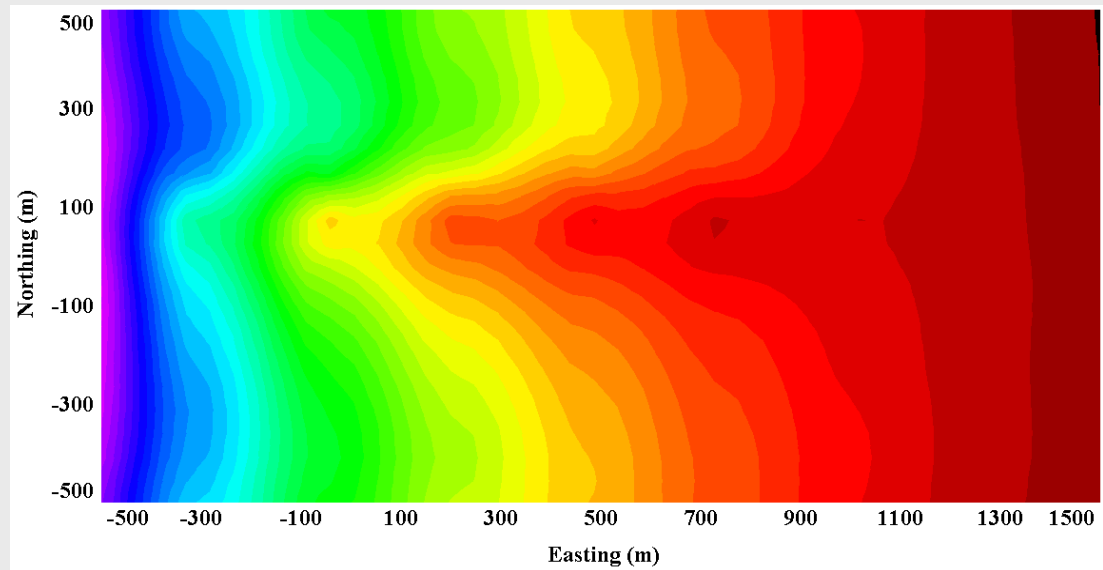
# Gridded predicted data VS “true” data



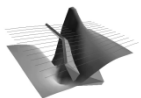
*“true”* data

1 kHz data

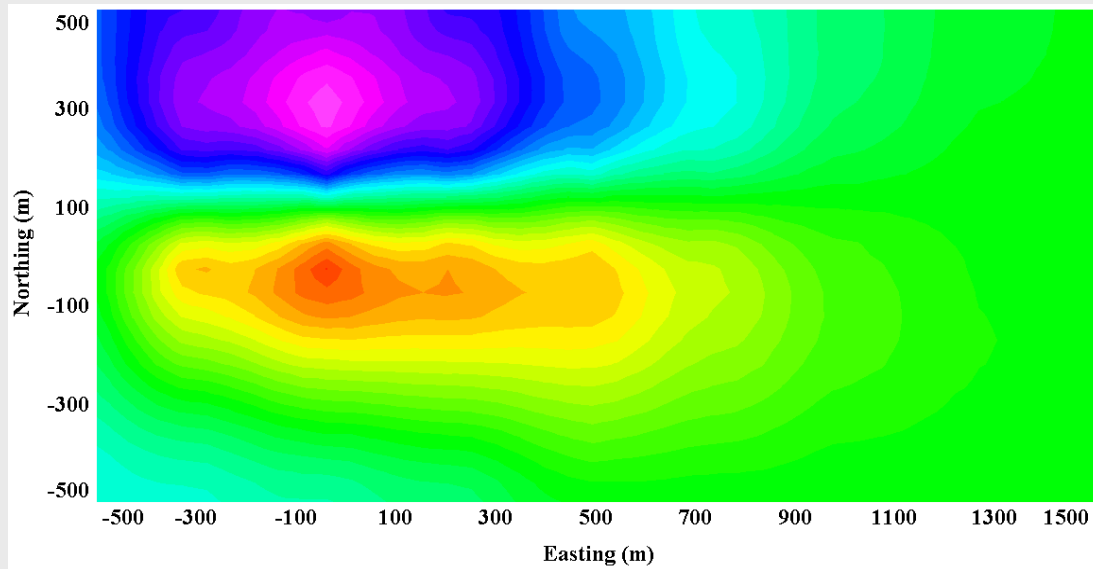
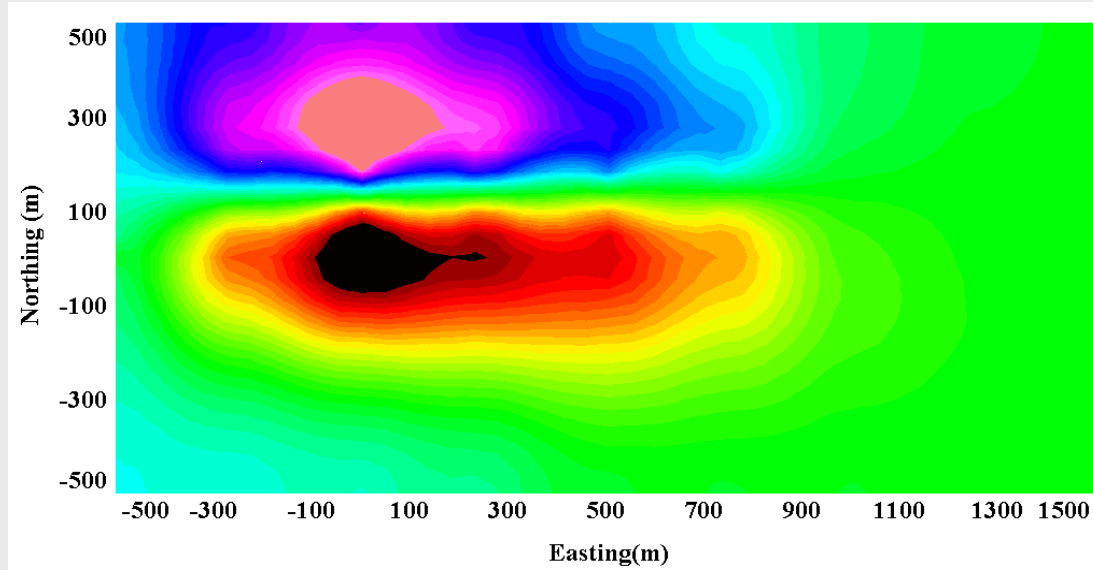
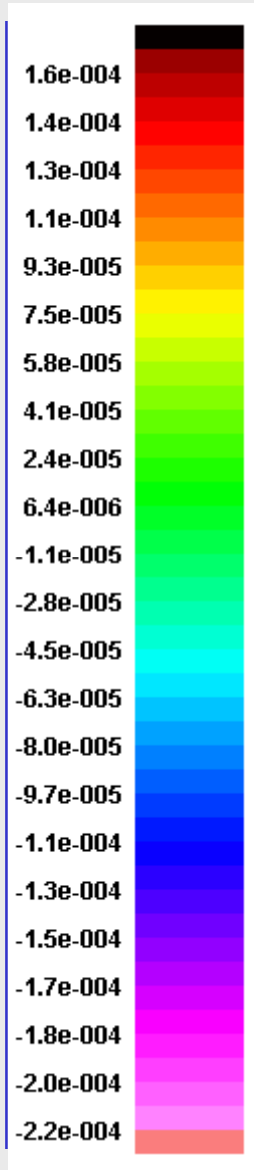
real part



predicted data



# Gridded predicted data VS “true” data

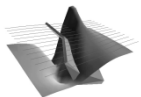


*”true”* data

1 kHz data

Imaginary part

predicted data



# Real data example

Current bipole

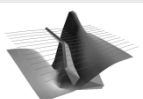
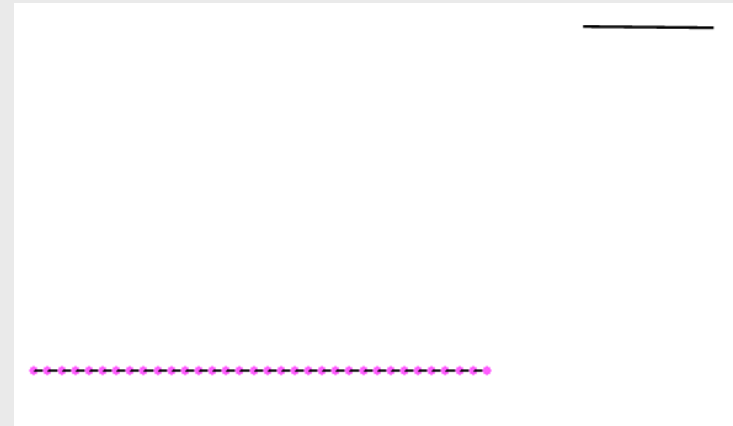
Transmitter is 8 km north and 500 m east of survey area and has a length of 1.2 km

**Survey: 1 line of length 1.6 km**

**Station separation: 50 m**

**34 stations**

- Ex and Hy
- 14 frequencies (Hz): 1, 4, 8, 16, 64, ..., 8192
- Ex: voltage bipole of length 50 m



# Inversion setting

## -regular grid

**3D inversion region: 1600 x 800 x 1000 m**

**Grid cell size: 25 x 800 x 50 m**

**Grid cell number: 64 x 1 x 20**

Each cell Sampled 8 in y direction

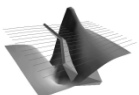
**Starting model:** uniform half-space of 50  $\Omega\text{m}$

**Constraints:**  $1 \leq \rho_i \leq 2000 \Omega\text{m}$

**11 Frequencies used (Hz):** from 8 to 128 Hz

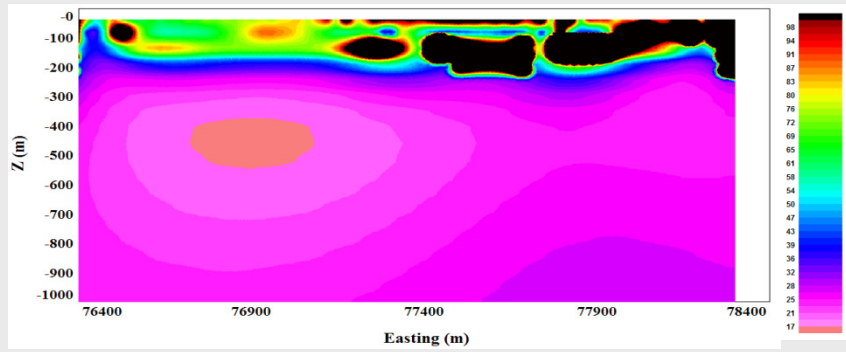
**smoothing coefficients:**

EW: 3, Vertical: 8

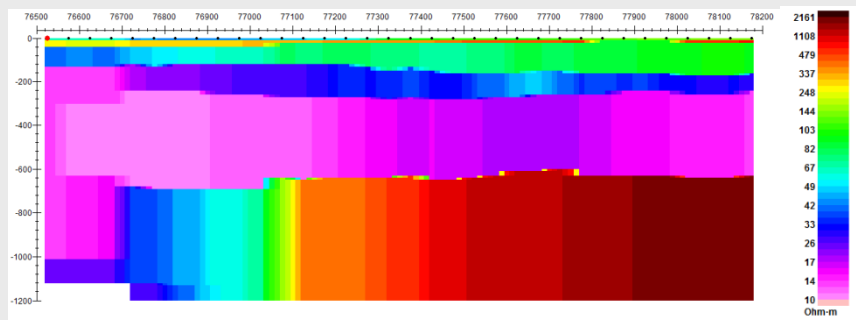




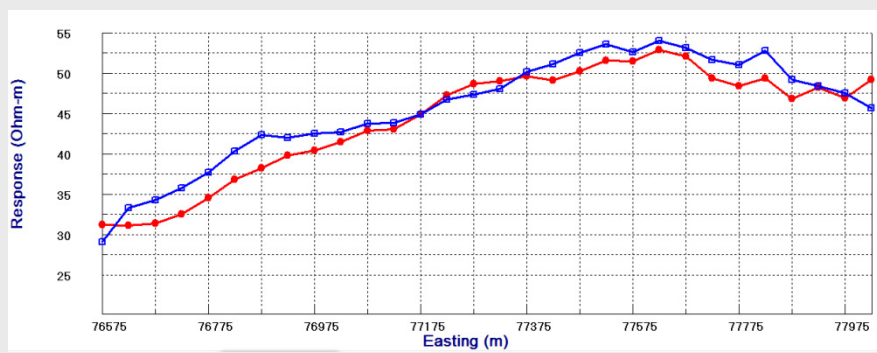
# Inversion results – on apparent resistivity



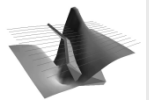
3d inversion model



1d inversion model



64 Hz apparent resistivity  
Red: observed data  
Blue: recovered data



# Conclusions and Future Work

- ❖ the resolution of the inversion can be dramatically improved by utilizing dipping and striking grid cells with the known orientation.
  - The resolution of the inverted results in the strike and dip directions can be easily controlled by the smoothing constraints in a model objective function.
  - the structure can be better represented with grid cells of the same orientation.
- ❖ The use of individual fields or the combined impedance ration provides more flexibility in structural determination as well as dealing with bad data.

## Future work

- To incorporate different strike and dip angles in regions of subsurface, we may divide the 3D inversion volume into sub-regions, each of which has its own strike and dip angle.

